Article

Dinitrogen Functionalization with Terminal Alkynes, Amines, and Hydrazines Promoted by [(η5-CMeH)Zr](η2,η2,η2-N): Observation of Side-On and End-On Diazenido Complexes in the Reduction of N2 to Hydrazine

Wesley H. Bernskoetter, Jaime A. Pool, Emil Lobkovsky, and Paul J. Chirik

J. Am. Chem. Soc., **2005**, 127 (21), 7901-7911• DOI: 10.1021/ja050387b • Publication Date (Web): 07 May 2005

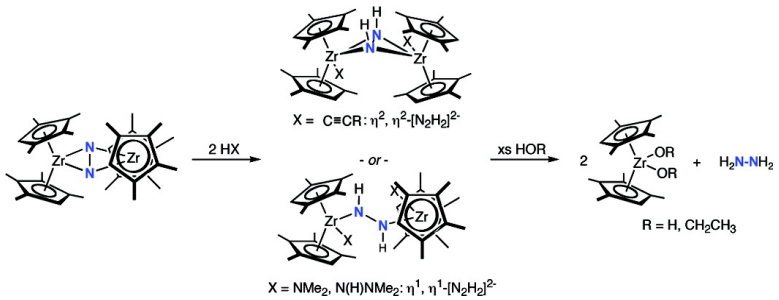

More About This Article

Additional resources and features associated with this article are available within the HTML version:

- Supporting Information
- Links to the 12 articles that cite this article, as of the time of this article download
- Access to high resolution figures
- Links to articles and content related to this article
- Copyright permission to reproduce figures and/or text from this article

View the Full Text HTML

J|A|C|S
ARTICLES
Published on Web 05/07/2005

Dinitrogen Functionalization with Terminal Alkynes, Amines, and Hydrazines Promoted by $[(\eta^5\text{-}C_5Me_4H)_2Zr]_2(\mu_2,\eta^2,\eta^2\text{-}N_2)$: Observation of Side-On and End-On Diazenido Complexes in the Reduction of N_2 to Hydrazine

Wesley H. Bernskoetter, Jaime A. Pool,† Emil Lobkovsky, and Paul J. Chirik*

Contribution from the Department of Chemistry and Chemical Biology, Baker Laboratory, Cornell University, Ithaca, New York 14853

Received January 20, 2005; E-mail: pc92@cornell.edu

Abstract: Functionalization of the N_2 ligand in the side-on bound dinitrogen complex, $[(\eta^5\text{-}C_5Me_4H)_2Zr]_2(\mu_2,\eta^2,\eta^2\text{-}N_2)$, has been accomplished by addition of terminal alkynes to furnish acetylide zirconocene diazenido complexes, $[(\eta^5\text{-}C_5Me_4H)_2Zr(C{\equiv}CR)]_2(\mu_2,\eta^2,\eta^2\text{-}N_2H_2)$ (R = ^{n}Bu, ^{t}Bu, Ph). Characterization of $[(\eta^5\text{-}C_5Me_4H)_2Zr(C{\equiv}CCMe_3)]_2(\mu_2,\eta^2,\eta^2\text{-}N_2H_2)$ by X-ray diffraction revealed a side-on bound diazenido ligand in the solid state, while variable-temperature ^{1}H and ^{15}N NMR studies established rapid interconversion between η^1,η^1 and η^2,η^2 hapticity of the $[N_2H_2]^{2-}$ ligand in solution. Synthesis of alkyl, halide, and triflato zirconocene diazenido complexes, $[(\eta^5\text{-}C_5Me_4H)_2ZrX]_2(\mu_2,\eta^1,\eta^1\text{-}N_2H_2)$ (X = Cl, I, OTf, CH_2Ph, CH_2SiMe_3), afforded η^1,η^1 coordination of the $[N_2H_2]^{2-}$ fragment both in the solid state and in solution, demonstrating that sterically demanding, in some cases π-donating, ligands can overcome the electronically preferred side-on bonding mode. Unlike $[(\eta^5\text{-}C_5Me_4H)_2ZrH]_2(\mu_2,\eta^2,\eta^2\text{-}N_2H_2)$, the acetylide and alkyl zirconocene diazenido complexes are thermally robust, resisting α-migration and N_2 cleavage up to temperatures of 115 °C. Dinitrogen functionalization with $[(\eta^5\text{-}C_5Me_4H)_2Zr]_2(\mu_2,\eta^2,\eta^2\text{-}N_2)$ was also accomplished by addition of proton donors. Weak Brønsted acids such as water and ethanol yield hydrazine and $(\eta^5\text{-}C_5Me_4H)_2Zr(OH)_2$ and $(\eta^5\text{-}C_5Me_4H)_2Zr(OEt)_2$, respectively. Treatment of $[(\eta^5\text{-}C_5Me_4H)_2Zr]_2(\mu_2,\eta^2,\eta^2\text{-}N_2)$ with $HNMe_2$ or H_2NNMe_2 furnished amido or hydrazido zirconocene diazenido complexes that ultimately produce hydrazine upon protonation with ethanol. These results contrast previous observations with $[(\eta^5\text{-}C_5Me_5)_2Zr(\eta^1\text{-}N_2)]_2(\mu_2,\eta^1,\eta^1\text{-}N_2)$ where loss of free dinitrogen is observed upon treatment with weak acids. These studies highlight the importance of cyclopentadienyl substituents on transformations involving coordinated dinitrogen.

Introduction

Dinitrogen functionalization promoted by soluble transition metal complexes continues to be actively investigated.[1] Paramount to this effort is the discovery of mild, energy-efficient methods for the construction of nitrogen−hydrogen bonds given both the industrial[2] and the biological[3] significance of ammonia. For well-defined, homogeneous metal dinitrogen complexes, the so-called "Chatt-cycle" is the most common and well-established method for N_2 reduction.[4] Classically, a weakly activated, zerovalent dinitrogen complex of molybdenum or tungsten, $[(R_3P)_4M(N_2)L]$ (L = N_2 or other neutral ligand), is treated with a mineral acid to yield N_2H_4 or NH_3.[5] Introduction of triamidoamine ligands with sterically demanding aryl substituents has allowed observation of many intermediates in the reduction cycle,[6] ultimately resulting in complexes that catalytically fix N_2 to ammonia by a series of successive proton and electron-transfer reactions.[7] Recently, this approach has been extended to cobalt and iron−dinitrogen complexes to affect C−N and C−Si bond formation.[8]

Electrophilic functionalization of strongly activated early transition metal complexes has also been used to prepare ammonia,[9] hydrazine,[10] and heterocycles[11] directly from N_2. Significantly, the reduced dinitrogen ligands in this class of molecule also open new pathways for nitrogen-element bond formation using nonpolar reagents.[12] Dinuclear tantalum and zirconium dinitrogen complexes supported by macrocyclic phosphine diamide ligands[13] have proven particularly interesting for this method of functionalization, resulting in the hydrosilation

† Current address: Chemistry Division, Los Alamos National Laboratory, Los Alamos, NM 87545.

(1) (a) MacKay, B. A.; Fryzuk, M. D. *Chem. Rev.* **2004**, *104*, 381. (b) Gambarotta, S.; Scott, J. *Angew. Chem., Int. Ed.* **2004**, *43*, 5298.
(2) Smil, V. *Enriching the Earth: Fritz Haber, Carl Bosch, and the Transformation of World Food Production*; MIT Press: Cambridge, MA, 2001.
(3) (a) Einsle, O.; Tezcan, F. A.; Andrade, S. L. A.; Schmid, B.; Yoshida, M.; Howard, J. B.; Rees, D. C. *Science* **2002**, *297*, 1696. (b) Burgess, B. K.; Lowe, D. J. *Chem. Rev.* **1996**, *96*, 2983.
(4) Chatt, J.; Dilworth, J. R.; Richards, R. L. *Chem. Rev.* **1978**, *78*, 589.
(5) Chatt, J.; Pearman, A. J.; Richards, R. L. *J. Chem. Soc., Dalton Trans.* **1977**, 1852.
(6) Yandulov, D. V.; Schrock, R. R. *J. Am. Chem. Soc.* **2002**, *124*, 6262.
(7) (a) Ritleng, V.; Yandulov, D. V.; Weare, W. W.; Schrock, R. R.; Hock, A. S.; Davis, W. M. *J. Am. Chem. Soc.* **2004**, *126*, 6150. (b) Yandulov, D. V.; Schrock, R. R. *Science* **2003**, *76*, 301.
(8) Betley, T. A.; Peters, J. C. *J. Am. Chem. Soc.* **2003**, *125*, 10782.
(9) (a) Vol'pin, M. E.; Shur, V. B. *Nature* **1966**, *209*, 1236. (b) Luneva, N. P.; Nikonova, L. A.; Shilov, A. E. *React. Kinet. Catal. Lett.* **1976**, *5*, 149. (c) Shestakov, A. F.; Shilov, A. E. *Kinet. Catal.* **2001**, *42*, 653.
(10) Manriquez, J. M.; Bercaw, J. E. *J. Am. Chem. Soc.* **1974**, *96*, 6229.
(11) Mori, M.; Akashi, M.; Hori, M.; Hori, K.; Nishida, M.; Sato, Y. *Bull. Chem. Soc. Jpn.* **2004**, *77*, 1655.

(Zr,[14] Ta[15]), hydroboration (Ta),[16] and even partial hydrogenation[13] of coordinated dinitrogen. Most recently, nitrogen−carbon bond formation by addition of terminal alkynes to the zirconium dinitrogen complex has been described, forming a bridging acetylide and a carbon-substituted hydrazido ligand.[17]

Our laboratory has been exploring the effect of cyclopentadienyl ligand substitution on the hapticity and reactivity of coordinated dinitrogen in low-valent group 4 metallocene complexes.[18] Whereas $[(\eta^5\text{-}C_5Me_5)_2Zr(\eta^1\text{-}N_2)]_2(\mu_2,\eta^1,\eta^1\text{-}N_2)$[10] and $[(\eta^5\text{-}C_5Me_5)(\eta^5\text{-}C_5Me_4H)Zr(\eta^1\text{-}N_2)]_2(\mu_2,\eta^1,\eta^1\text{-}N_2)$[19] contain weakly activated "end-on" coordinated dinitrogen ligands that are readily displaced by dihydrogen, the octamethyl-substituted zirconocene dinitrogen complex, $[(\eta^5\text{-}C_5Me_4H)_2Zr]_2(\mu_2,\eta^2,\eta^2\text{-}N_2)$ (**1**), has a side-on bound N_2 ligand with an elongated N−N bond of 1.377(3) Å. Exposure of **1** to a dihydrogen atmosphere resulted in nitrogen−hydrogen bond formation to afford $[(\eta^5\text{-}C_5Me_4H)_2ZrH]_2(\mu_2,\eta^2,\eta^2\text{-}N_2H_2)$ (**2**), which upon warming to 85 °C under additional H_2 produced small quantities of free ammonia (eq 1).[20]

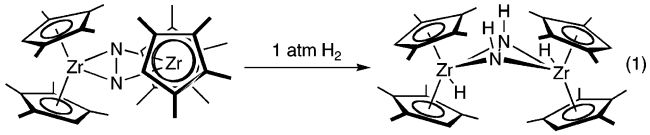

1 **2**

Subsequent isotopic labeling and computational studies established that the unique hydrogenation reactivity of **1** stems from the "twisted" ground-state structure of the dinuclear zirconium complex.[19] As the dihedral angle between zirconocene wedges approaches orthogonality, the $1a_1$ orbitals of the two metals can effectively overlap with the perpendicular lobes of the π^* molecular orbitals of the η^2-N_2 ligand, thereby facilitating the addition of dihydrogen.[18] In light of these observations, we became interested in the possibility of dinitrogen functionalization by both electrophilic and cycloaddition pathways. Here, we describe formation of N−H bonds by addition of terminal alkynes, dimethylamine, and *N*,*N*-dimethylhydrazine to **1** and explore the mechanism of N_2 functionalization. The solution dynamics, molecular structures, and coordination preferences of the resulting zirconocene diazenido complexes are also reported. These studies underscore the significance of both cyclopentadienyl ligand substituents and N_2 hapticity on N−H bond forming reactions involving coordinated dinitrogen.

Results and Discussion

Dinitrogen Functionalization with Terminal Alkynes. Because $[(\eta^5\text{-}C_5Me_4H)_2Zr]_2(\mu_2,\eta^2,\eta^2\text{-}N_2)$ (**1**) undergoes facile addition of dihydrogen to afford the side-on bound hydrido zirconocene diazenido complex, $[(\eta^5\text{-}C_5Me_4H)_2ZrH]_2(\mu_2,\eta^2,\eta^2\text{-}N_2H_2)$ (**2**), dinitrogen functionalization with other molecules that could possibly undergo similar cycloaddition-type chemistry was investigated. Alkynes are attractive candidates given their well-documented reaction chemistry with group 4 imido complexes.[21,22] While cycloaddition to yield azametallacycles is frequently observed,[23,24] formal C−H activation of terminal alkynes by the base-free titanocene imido, $(\eta^5\text{-}C_5Me_5)_2Ti{=}NPh$, affords the corresponding anilido acetylide species, $(\eta^5\text{-}C_5Me_5)_2Ti(N(Ph)H)C{\equiv}CR$ (R = Ph, $SiMe_3$),[25] demonstrating the potential utility of these substrates to promote N−H bond formation from coordinated dinitrogen.

Addition of 2 equiv of a terminal acetylene to **1** at ambient temperature furnished the acetylide zirconocene diazenido compounds, $[(\eta^5\text{-}C_5Me_4H)_2Zr(C{\equiv}CR)]_2(\mu_2,\eta^2,\eta^2\text{-}N_2H_2)$ (R = $(CH_2)_3CH_3$, **3**; CMe_3, **4**; C_6H_5, **5**), arising from formal activation of the alkyne C−H bond by the dinitrogen complex (eq 2). Complete conversion to products is observed immediately upon thawing frozen benzene-d_6 solutions. Formation of two new N−H bonds from alkyne addition to a dinitrogen complex is, to our knowledge, unprecedented and contrasts the reactivity of a bis(phosphine)diamide-ligated zirconium dinitrogen complex where cycloaddition yields a new nitrogen−carbon bond and a bridging acetylide.[17] The different products observed from the two types of zirconium−N_2 complexes are most likely steric in origin, where the more hindered zirconocene system favors C−H activation over cycloaddition. Similar observations have been made in permethyltitanocene oxo chemistry, where equilibration of oxometallocyclobutanes to the thermodynamically favored and sterically less congested hydroxide acetylide complexes occurs.[26] This rationale has also been invoked to explain the observed anilido acetylide products formed from addition of terminal alkynes to the permethyltitanocene imido complex mentioned above.[25]

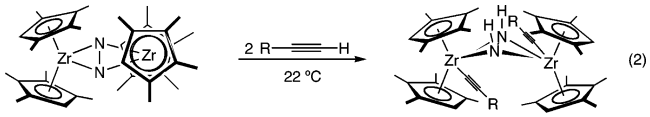

1

R = $(CH_2)_3CH_3$, **3**
= CMe_3, **4**
= C_6H_5, **5**

The functionalized products, **3**−**5**, were characterized by a combination of multinuclear (^1H, ^{13}C, ^{15}N) NMR experiments, IR spectroscopy, elemental analysis, and, in one case, **4**, X-ray diffraction. At 23 °C in benzene-d_6, the ^1H NMR spectra for **3**−**5** display sharp peaks for the acetylide resonances and one sharp cyclopentadienyl methyl group. The other cyclopentadienyl methyl peaks as well as the cyclopentadienyl hydrogen

(12) Protonation of group 6 dinitrogen complexes using H_2 as the hydrogen source has been accomplished by pre-coordination to ruthenium or metal sulfide complexes. See: (a) Ru: Nishibayashi, Y.; Iwai, S.; Hidai, M. *Science* **1998**, *279*, 540. (b) Molybdenum-sulfides: Nishibayashi, Y.; Wakiji, I.; Hirata, K.; DuBois, M. R.; Hidai, M. *Inorg. Chem.* **2001**, *40*, 578. (c) Iron-sulfides: Nishibayashi, Y.; Iwai, S.; Hidai, M. *J. Am. Chem. Soc.* **1998**, *120*, 10559.
(13) Fryzuk, M. D. *Chem. Rec.* **2003**, *3*, 2.
(14) Fryzuk, M. D.; Love, J. B.; Rettig, S. J. *Science* **1997**, *275*, 1445.
(15) Fryzuk, M. D.; MacKay, B. A.; Patrick, B. O. *J. Am. Chem. Soc.* **2003**, *125*, 3234.
(16) Fryzuk, M. D.; MacKay, B. A.; Johnson, S. A.; Patrick, B. O. *Angew. Chem., Int. Ed.* **2002**, *41*, 3709.
(17) Morello, L.; Love, J. B.; Patrick, B. O.; Fryzuk, M. D. *J. Am. Chem. Soc.* **2004**, *126*, 9480.
(18) Pool, J. A.; Chirik, P. J. *Can. J. Chem.* **2005**, *83*, 286.
(19) Pool, J. A.; Bernskoetter, W. H.; Chirik, P. J. *J. Am. Chem. Soc.* **2004**, *126*, 14326.
(20) Pool, J. A.; Lobkovsky, E.; Chirik, P. J. *Nature* **2004**, *427*, 527.
(21) (a) Mountford, P. *Chem. Commun.* **1997**, 2127. (b) Duncan, A. P.; Bergman, R. G. *Chem. Rec.* **2002**, *2*, 431.
(22) Schaller, C. P.; Cummins, C. C.; Wolczanski, P. T. *J. Am. Chem. Soc.* **1996**, *118*, 591.
(23) (a) Harlan, C. J.; Tunge, J. A.; Bridgewater, B. M.; Norton, J. R. *Organometallics* **2000**, *19*, 2365. (b) Harlan, C. J.; Hascall, T.; Fujita, E.; Norton, J. R. *J. Am. Chem. Soc.* **1999**, *121*, 7274. (c) Harlan, C. J.; Bridgewater, B. M.; Hascall, T.; Norton, J. R. *Organometallics* **1999**, *18*, 3827.
(24) (a) Walsh, P. J.; Hollander, F. J.; Bergman, R. G. *Organometallics* **1993**, *12*, 3705. (b) Walsh, P. J.; Hollander, F. J.; Bergman, R. G. *J. Am. Chem. Soc.* **1988**, *110*, 8729.
(25) Polse, J. L.; Anderson, R. A.; Bergman, R. G. *J. Am. Chem. Soc.* **1998**, *120*, 13405.
(26) Polse, J. L.; Andersen, R. A.; Bergman, R. G. *J. Am. Chem. Soc.* **1995**, *117*, 5393.

Table 1. Selected Infrared Spectroscopic Data for **3**−**5** Recorded in KBr

compound	R	ν N–H (cm^{-1})	ν C≡C (cm^{-1})
3	$CH_2(CH_2)_2CH_3$	3453	2093
4	CMe_3	3582	2079
5	C_6H_5	3297	2079

are significantly broadened. Likewise, a resonance attributable to the hydrogen attached to the nitrogen is not observed at this temperature. These data, in combination with more detailed variable-temperature studies (vide infra), are consistent with a dynamic process where the diazenido ligand is interchanging between η^1,η^1 and η^2,η^2 coordination on the time scale of the NMR experiment.

Verification of N−H bond formation was provided by solid-state (KBr) infrared spectroscopy. Spectra of **3**−**5** exhibited broad peaks between 3297 and 3582 cm^{-1} (Table 1) attributed to N−H stretches. Confirmation of these assignments was obtained by preparation of $[(\eta^5\text{-}C_5Me_4H)_2Zr(C{\equiv}C^nBu)]_2(\mu_2,\eta^2,\eta^2\text{-}N_2D_2)$ (**3-*d*$_2$**), in which the N−D stretch shifts to 2441 cm^{-1}, in excellent agreement with the prediction made by the harmonic oscillator model. In addition to the N−H peaks, diagnostic bands[26,27] centered between 2079 and 2093 cm^{-1} are observed for the terminal acetylide ligands (Table 1).

The solid-state structure of **4** was elucidated by single crystal X-ray diffraction, and a representation of the molecule is shown in Figure 1. Selected bond distances and angles are reported in Table 2. The diffraction data were of sufficient quality such that all of the hydrogens, including those attached to the nitrogens, were located and freely refined, thus providing unambiguous assignment of the product. In the solid state, the core of the molecule contains a side-on bound diazenido ligand that is puckered by 45.54(5)° due to the pyramidalization of the nitrogens, similar to the geometry of **2**.[20] The acetylide ligands are oriented in a transoid fashion to minimize steric interactions between the *tert*-butyl substituents. While a steric argument seems reasonable, it should be noted that a similar transoid arrangement is also observed in **2**,[20] where small hydride ligands are present in the metallocene wedge.

Also in agreement with the solid-state structure of **1** and **2**[20] is the observation of a significant twisting of the dimer in **4** as evidenced by a dihedral angle of 73.7° formed between the planes defined by the zirconium and the cyclopentadienyl centroids. The N−N bond length of 1.454(2) Å is consistent with reduction of coordinated dinitrogen to a diazenido ligand and is comparable to the bond lengths of 1.46 and 1.457(3) Å observed in hydrazine[28] and **2**,[20] respectively. Also consistent with a $[N_2H_2]^{2-}$ ligand[29] is the observation of an asymmetric core with short Zr−N bonds of 2.190(2) and 2.192(2) Å for the anionic, "X-type" interactions and longer 2.337(2) and 2.328(2) Å distances for the neutral, "L-type" Zr−N bonds.

The hydrido zirconocene diazenido, **2**, is known to undergo α-hydrogen migration concomitant with H_2 loss and N_2 cleavage upon warming to 45 °C.[19,20] This unusual behavior prompted investigation of the thermal stability of **3**−**5** with the goal of forming a nitrogen−carbon bond and comparing the energetic requirements of the two processes. All three acetylide-substituted

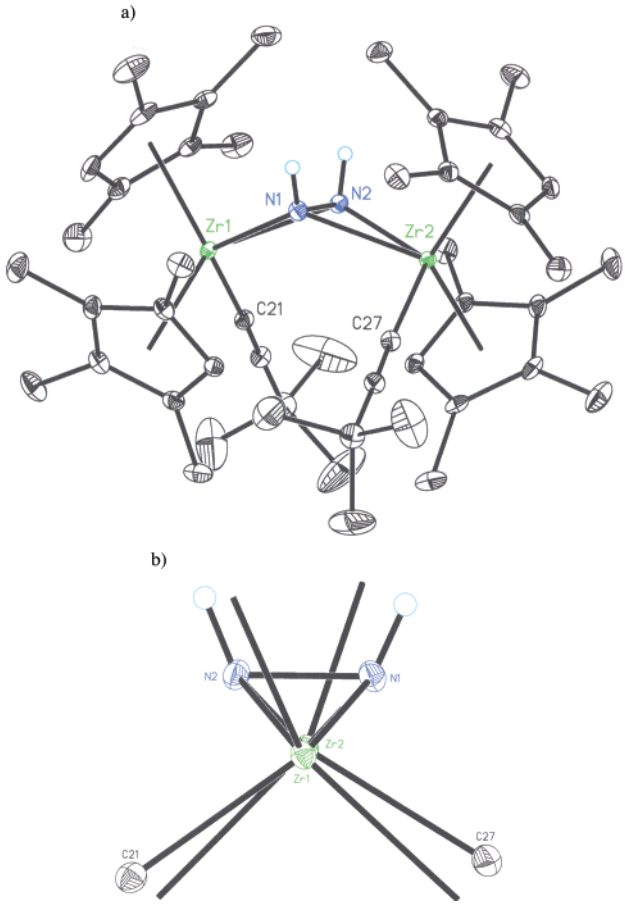

Figure 1. (a) Molecular structure of **4** at 30% probability ellipsoids. Hydrogen atoms, except for those attached to nitrogen, are omitted for clarity. (b) View of the core of the molecule.

Table 2. Selected Bond Distances (Å) and Angles (°) for **4**

Zr(1)−N(1)	2.190(2)
Zr(1)−N(2)	2.337(2)
Zr(2)−N(1)	2.328(2)
Zr(2)−N(2)	2.192(2)
Zr(1)−C(21)	2.251(2)
Zr(2)−C(27)	2.267(2)
N(1)−N(2)	1.454(2)
C(21)−C(22)	1.216(2)
C(27)−C(28)	1.215(2)
Zr(1)−N(1)−Zr(2)	122.93(7)
Zr(1)−N(2)−Zr(2)	122.39(7)
N(1)−N(2)−Zr(1)	65.84(8)
N(1)−N(2)−Zr(2)	76.39(8)
N(1)−Zr(2)−N(2)	37.29(5)
Zr(1)−C(21)−C(22)	177.66(16)
Zr(2)−C(27)−C(28)	176.31(16)

zirconocene diazenido complexes are thermally robust; heating sealed NMR tubes containing benzene-d_6 solutions of **3**−**5** to 115 °C for several days produced no observable change in the ^{1}H NMR spectra. Decomposition by loss of free alkyne and formation of unidentified zirconium compounds is observed upon heating to 160 °C. Although an sp hybridized acetylide

(27) Pellny, P.-M.; Kirchbauer, F. G.; Burlakov, V. V.; Baumann, W.; Spannenberg, A.; Rosenthal, U. *Chem.-Eur. J.* **2000**, *6*, 81.
(28) Fryzuk, M. D.; Johnson, S. A. *Coord. Chem. Rev.* **2000**, *200*, 379.
(29) For examples of complexes with $[N_2H_2]^{2-}$ ligands: (a) Churchill, M. R.; Li, Y.-J.; Blum, L. *Organometallics* **1984**, *3*, 109. (b) Blum, L.; Williams, I. D.; Schrock, R. R. *J. Am. Chem. Soc.* **1984**, *106*, 8316. (c) González-Maupoey, M.; Rodríguez, G. M.; Cuenca, T. *Eur. J. Inorg. Chem.* **2002**, 2057.

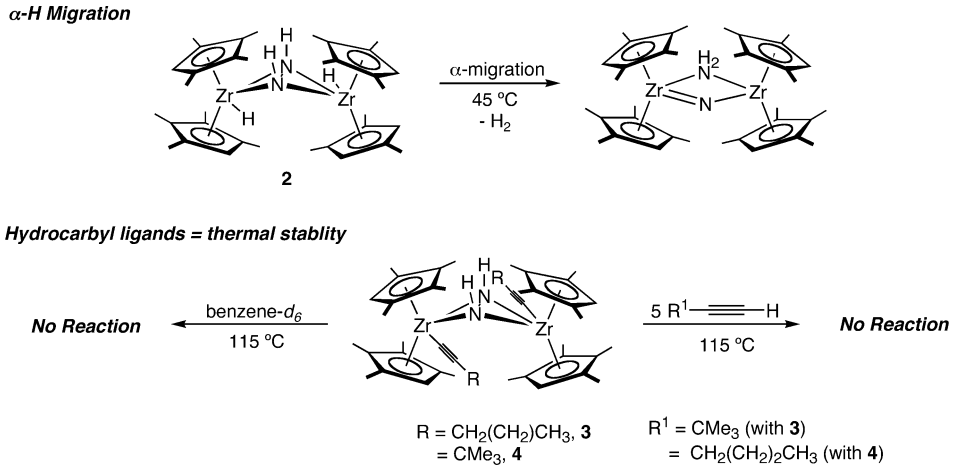

Figure 2. Thermal stability of acetylide zirconocene diazenido complexes.

ligand would require the least orbital reorganizational energy of any hydrocarbyl for α-migration, the barrier is significantly higher than the corresponding hydrogen migration and is not observed under typical thermolysis conditions. A combination of experimental and computational studies from Wolczanski have shown that 1,2-elimination of alkyne from (^{t}Bu$_3$SiNH)$_3$Zr-(C≡CR) was inhibited by a high kinetic barrier and that [2+2] cycloaddition and reversion pathways were energetically competent, accounting for associative exchange of the acetylide ligand with free alkyne.[22] For zirconocene diazenido compounds, previous work from our laboratory with isotopologues of **2** have shown the 1,2-elimination of dihydrogen precedes α-migration, suggesting that the lack of reactivity observed with **3**−**5** may be a result of a high kinetic barrier associated with elimination of alkyne.

Examination of potential acetylide exchange reactions also supports these observations. Thermolysis of **3** in benzene-d_6 at 115 °C in the presence of 5 equiv of HC≡CCMe$_3$ produced no reaction over the course of days (Figure 2). Likewise, heating **4** to 115 °C in the presence of 1-hexyne also did not yield new products, further demonstrating the thermal stability of these molecules. Importantly, these results establish that a competitive [2+2] cycloreversion/addition pathway that can interchange alkynes is also not operative as is the case with other group 4 metallacyclobutenes[21,26] and (^{t}Bu$_3$SiNH)$_3$Zr(C≡CR) compounds.[22]

Evidence that terminal alkynes can participate in protonolysis/σ-bond metathesis pathways has been obtained by addition of terminal alkynes to [(η^5-C$_5$Me$_4$H)$_2$ZrD]$_2$(μ_2,η^2,η^2-N$_2$D$_2$) (**2-*d*$_4$**).[20] Gentle warming of a benzene-d_6 solution of **2-*d*$_4$** to 50 °C in the presence of an excess of HC≡CCMe$_3$ resulted in loss of HD and formation of [(η^5-C$_5$Me$_4$H)$_2$Zr(C≡CCMe$_3$)]$_2$(μ_2,η^2,η^2-N$_2$D$_2$) (**4-*d*$_2$**) (eq 3). Importantly, no evidence for the perproteo isotopologue, **4**, was obtained. Thus, protonolysis/σ-bond metathesis is favored over the 1,2-elimination/addition sequence. Significantly, previous studies with **2** and **2-*d*$_4$** have shown that 1,2-elimination of dihydrogen is facile at 50 °C.[19]

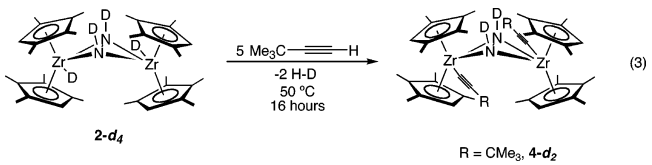

(3)

Preparation of Halide and Alkyl Zirconocene Diazenido Complexes and Coordination Preferences of the [N$_2$H$_2$]$^{2-}$ Core. Because of the importance of the diazenido complexes in dinitrogen functionalization and cleavage processes, the coordination preferences of the [N$_2$H$_2$]$^{2-}$ ligand were explored in more detail. Ideally, establishing structure−reactivity relationships would provide new opportunities for dinitrogen functionalization. We hypothesized that introduction of sterically demanding or π-donating (or both) "spectator" ligands in the zirconocene wedge would disfavor side-on coordination of the [N$_2$H$_2$]$^{2-}$ fragment and allow isolation of η^1,η^1 diazenido complexes. Treatment of **2** with a slight excess of MeI induced loss of 2 equiv of methane and furnished dark purple crystals of [(η^5-C$_5$Me$_4$H)$_2$ZrI]$_2$(μ_2,η^1,η^1-N$_2$H$_2$) (**6**) (eq 4). Preparation of the isotopologues, [(η^5-C$_5$Me$_4$H)$_2$ZrI]$_2$(μ_2,η^1,η^1-N$_2$D$_2$) (**6-*d*$_2$**) and [(η^5-C$_5$Me$_4$H)$_2$ZrI]$_2$(μ_2,η^1,η^1-^{15}N$_2$H$_2$) (**6-^{15}N**), was accomplished by addition of CH$_3$I to **2-*d*$_4$** and **2-^{15}N**,[20] respectively.

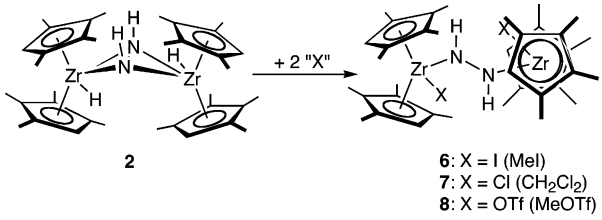

(4)

The ^{1}H NMR spectrum of **6** recorded in benzene-d_6 at 23 °C exhibits the expected number of cyclopentadienyl ligand resonances for a static molecule where the two halves of the dimer are related by symmetry. The N−H resonance is shifted substantially downfield to 8.90 ppm, in contrast to **2**, where this peak is centered at 0.83 ppm. This suggests a different magnetic environment and hence a different hapticity for the diazenido ligand. Spectra of two isotopologues confirmed this assignment. The ^{2}H NMR spectrum of **6-*d*$_2$** in benzene exhibits a single peak centered at 8.90 ppm, while in the ^{1}H NMR spectrum of **6-^{15}N** this resonance appears as an AA′XX′ spin system. Simulation of the data[30] (Figure S1, Supporting Information) provided the following coupling constants: $^3J_{H-H}$: 9.4 Hz, $^1J_{N-H}$: 72.6 Hz, $^2J_{N-H}$: −3.1 Hz, and $^1J_{N-N}$: 21.6 Hz. Infrared spectra of benzene-d_6 solutions also supported the

(30) Marat, K. *Spinworks*; University of Manitoba: Manitoba, Canada, 2004.

Table 3. ^{1}H and ^{15}N NMR Chemical Shifts of Selected Zirconocene Diazenido Complexes in Benzene-d_6 at 22 °C

compound	δ N–H (ppm)	δ ^{15}N (ppm)
$[(\eta^5\text{-}C_5Me_4H)_2ZrH]_2(\mu_2,\eta^2,\eta^2\text{-}N_2H_2)$ (**2**)	0.83	74.6[c] 78.7[b]
$[(\eta^5\text{-}C_5Me_4H)_2Zr(C{\equiv}C^nBu)]_2(\mu_2,\eta^2,\eta^2\text{-}N_2H_2)$ (**3**)	2.65[a] 5.00[b]	
$[(\eta^5\text{-}C_5Me_4H)_2Zr(C{\equiv}C^tBu)]_2(\mu_2,\eta^2,\eta^2\text{-}N_2H_2)$ (**4**)	4.80[b]	86.0[c] 224.4[d]
$[(\eta^5\text{-}C_5Me_4H)_2ZrI]_2(\mu_2,\eta^1,\eta^1\text{-}N_2H_2)$ (**6**)	8.90	285.9
$[(\eta^5\text{-}C_5Me_4H)_2ZrCl]_2(\mu_2,\eta^1,\eta^1\text{-}N_2H_2)$ (**7**)	8.91	
$[(\eta^5\text{-}C_5Me_4H)_2Zr(CH_2Ph)]_2(\mu_2,\eta^1,\eta^1\text{-}N_2H_2)$ (**9**)	8.14	
$[(\eta^5\text{-}C_5Me_4H)_2Zr(CH_2SiMe_3)]_2(\mu_2,\eta^1,\eta^1\text{-}N_2H_2)$ (**11**)	7.93	
$[(\eta^5\text{-}C_5Me_4H)_2Zr(NMe_2)]_2(\mu_2,\eta^1,\eta^1\text{-}N_2H_2)$ (**14**)	8.21	
$[(\eta^5\text{-}C_5Me_4H)_2Zr(NHNMe_2)]_2(\mu_2,\eta^1,\eta^1\text{-}N_2H_2)$ (**15**)	7.03 3.58[e]	

[a] Determined from ^{2}H NMR in benzene. [b] Spectrum recorded at 75 °C in toluene-d_8. [c] Spectrum recorded at −78 °C in toluene-d_8. [d] Spectrum recorded at 115 °C in toluene-d_8. [e] N−H on the terminal hydrazido ligand.

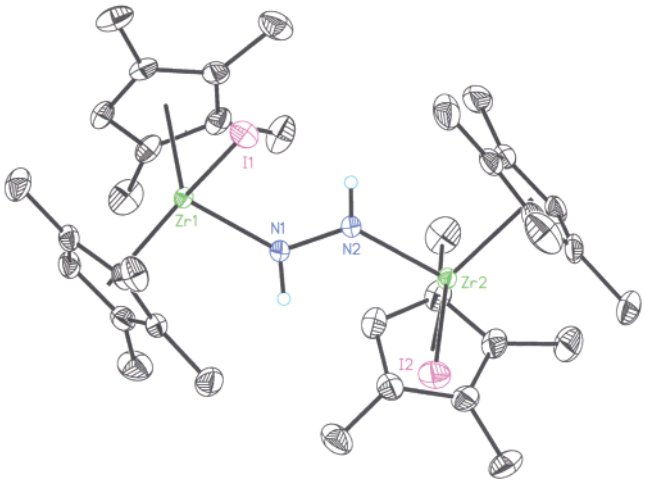

Figure 3. Molecular structure of **6** at 50% probability ellipsoids. Hydrogen atoms, except for those attached to nitrogen, are omitted for clarity.

presence of N−H bonds, exhibiting a broad N−H stretch centered at 3237 cm^{-1} which shifts appropriately to 2313 cm^{-1} for **6-*d*$_2$**.

The ^{15}N NMR spectrum of **6-^{15}N** contains a single resonance centered at 285.9 ppm. A collection of ^{1}H and ^{15}N chemical shifts of the diazenido ligands are reported in Table 3 and provide a convenient diagnostic tool for identification of the hapticity of the $[N_2H_2]^{2-}$ core. In general, η^1,η^1-$[N_2H_2]^{2-}$ ligands exhibit a downfield N−H resonance in the ^{1}H NMR spectrum, in the region of 7−9 ppm, whereas those which are side-on coordinated appear upfield around 1 ppm. While the data are limited, a similar trend is observed by ^{15}N NMR spectroscopy, where end-on diazenido ligands have downfield chemical shifts as compared to their side-on counterparts.

Confirmation of the η^1,η^1 hapticity of the diazenido ligand in **6** was provided by X-ray diffraction. Single crystals were obtained from slow evaporation of a benzene solution of **6**, and the solid-state structure is shown in Figure 3 with selected bond distances and angles reported in Table 4. The data were of sufficient quality such that all of the hydrogens, including those attached to nitrogen, were located and freely refined. Despite the change in hapticity, the N−N bond length of 1.414(3) Å in the diazenido ligand is comparable to the distances of 1.457(3) and 1.454(2) Å found in **2**[20] and **4**, respectively, that contain

Table 4. Selected Bond Distances (Å) and Angles (°) for **6** and **7**

	6	7
Zr(1)−N(1)	2.085(2)	2.0721(12)
Zr(1)−N(2)	2.083(2)	2.0645(12)
Zr(1)−X(1)[a]	2.8871(5)	2.4731(3)
Zr(2)−X(2)	2.8712(6)	2.4906(4)
N(1)−N(2)	1.414(3)	1.4173(15)
N(1)−H(1N)	0.89(3)	0.90(2)
N(2)−H(2N)	0.88(3)	0.86(2)
N(1)−Zr(1)−X(1)	90.61(6)	93.27(3)
N(2)−Zr(2)−X(2)	93.23(6)	96.94(3)
N(1)−N(2)−Zr(2)	132.35(16)	147.17(9)
N(2)−N(1)−Zr(1)	131.94(15)	126.53(9)
H(1N)−N(1)−N(2)	104.1(18)	108.0(11)
H(2N)−N(2)−N(1)	106(2)	102.9(13)
H(1N)−N(1)−Zr(1)	121.9(18)	125.2(11)
H(2N)−N(2)−Zr(2)	121(2)	108.3(13)

[a] X = I (**6**); Cl (**7**).

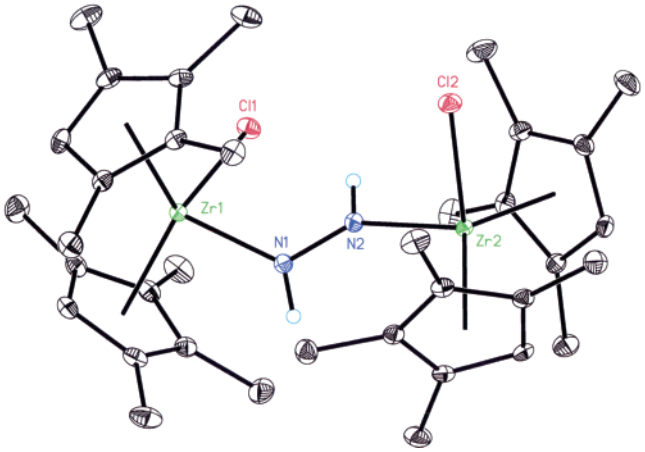

Figure 4. Molecular structure of **7** at 30% probability ellipsoids. Hydrogen atoms, except for those attached to nitrogen, are omitted for clarity.

η^2,η^2 bound $[N_2H_2]^{2-}$ ligands. The two zirconocene portions of the molecule are twisted with respect to one another, forming a dihedral angle of 76.7° between the planes formed from the metal and the two centroids of the cyclopentadienyl ligands. The change in hapticity of the diazenido ligand in **6** could be a consequence of the sterically demanding iodide ligand, inhibiting η^2,η^2 coordination of the $[N_2H_2]^{2-}$ fragment. It should also be noted that iodide could also serve as a π-donor and a combination of the effects is most likely responsible for the observed hapticity change.

To further explore the origin of the change in coordination mode of the diazenido ligand, synthesis of the corresponding dichloride complex, $[(\eta^5\text{-}C_5Me_4H)_2ZrCl]_2(N_2H_2)$, was targeted. Treatment of **2** with allyl chloride, benzyl chloride, trityl chloride, and methyl chloride all produced no reaction, while addition of protic reagents such as pyridinium hydrogen chloride or triethylammonium chloride resulted in conversion to the zirconocene dichloride, $(\eta^5\text{-}C_5Me_4H)_2ZrCl_2$, with loss of N_2H_4 (vide infra). However, simply stirring **2** in dichloromethane at 23 °C resulted in chlorine atom abstraction and furnished $[(\eta^5\text{-}C_5Me_4H)_2ZrCl]_2(\mu_2,\eta^1,\eta^1\text{-}N_2H_2)$ (**7**) in high yield (eq 4). As with **6**, the crystal structure (Figure 4, Table 4) and the observation of a downfield N−H resonance at 8.91 ppm (Table 3) establish end-on coordination of the diazenido ligand for **7** both in the solid state and in solution.

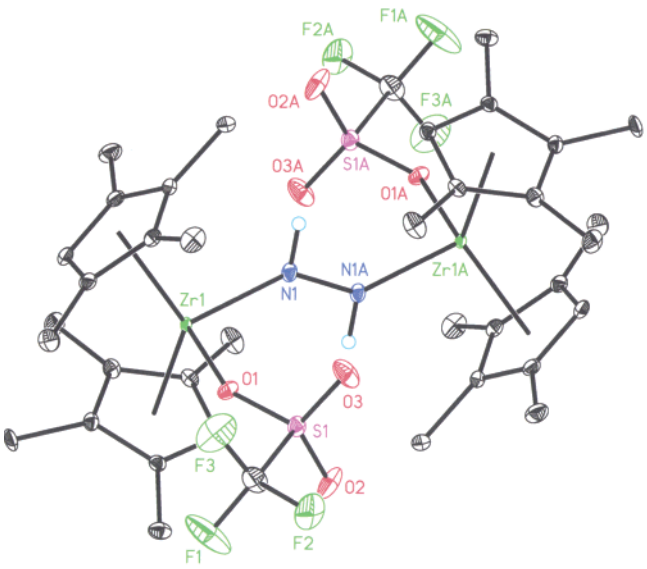

Figure 5. Molecular structure of **8** at 30% probability ellipsoids. Hydrogen atoms, except for those attached to nitrogen, are omitted for clarity.

Table 5. Selected Bond Distances (Å) and Angles (°) for **8**

Zr(1)−N(1)	2.086(3)
Zr(1)−O(1)	2.213(2)
N(1)−N(1A)	1.413(7)
N(1)−Zr(1)−O(1)	97.24(11)
N(1A)−N(1)−Zr(1)	137.2(3)

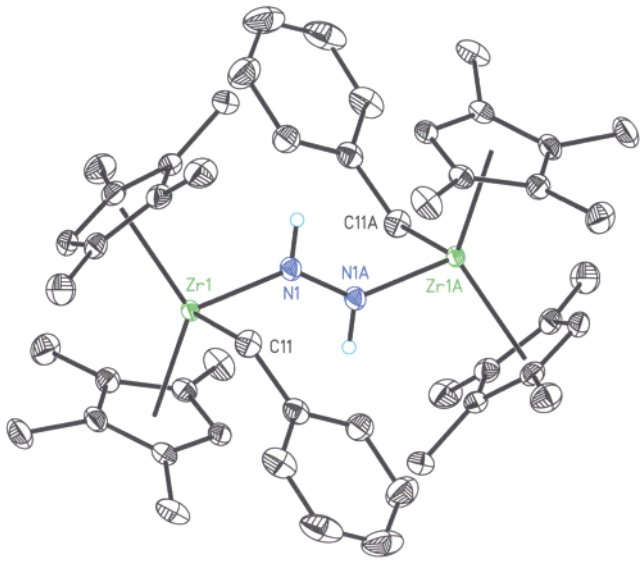

Figure 6. Molecular structure of **9** at 50% probability ellipsoids. Hydrogen atoms, except for those attached to nitrogen, are omitted for clarity.

Table 6. Selected Bond Distances (Å) and Angles (°) for **9**

Zr(1)−N(1)	2.0975(14)
Zr(1)−C(11)	2.3700(19)
N(1)−N(1A)	1.420(3)
N(1)−Zr(1)−C(11)	94.25(6)
N(1A)−N(1)−Zr(1)	137.62(15)

Synthesis of a similar triflato zirconocene diazenido complex, $[(\eta^5\text{-}C_5Me_4H)_2ZrOTf]_2(\mu_2,\eta^1,\eta^1\text{-}N_2H_2)$ (**8**), was accomplished by addition of 2 equiv of methyl triflate to **2** (eq 4). Unlike **6** and **7**, this complex is insoluble in common organic solvents prohibiting characterization by NMR spectroscopy. However, the solid-state (KBr) infrared spectrum of **8** contains a broad N−H stretch centered at 3351 cm^{-1}, which shifts appropriately to 2482 cm^{-1} upon preparation of **8-*d*$_2$**. In addition, a band centered at 1336 cm^{-1} for the triflato ligand was also observed.

Slow diffusion of methyl triflate into a benzene solution of **2** produced single crystals of **8** suitable for X-ray diffraction. The molecular structure of the compound is presented in Figure 5, and selected bond distances and angles are reported in Table 5. In the crystal structure, the molecule contains an inversion center that relates the two halves of the dimer and the transoid triflato ligands. As with **6**, an end-on diazenido ligand is observed with a typical N−N bond length of 1.413(7) Å.

Both **6** and **8** have proven to be useful synthons for alkyl zirconocene diazenido complexes. These molecules were of interest for structural comparison to the acetylide zirconocene diazenido complexes as well as for their potential utility to form nitrogen−carbon bonds by α-migration. Alkylation of **6** with 2 equiv of KCH_2Ph in diethyl ether afforded, after filtration and recrystallization, a red powder identified as $[(\eta^5\text{-}C_5Me_4H)_2Zr(CH_2Ph)]_2(\mu_2,\eta^1,\eta^1\text{-}N_2H_2)$ (**9**) in moderate yield (eq 5). In addition to the expected number of cyclopentadienyl ligand resonances, the ^{1}H NMR spectrum of **9** displays a downfield shifted N−H resonance at 8.14 ppm, consistent with end-on coordination of the diazenido ligand. As with the acetylide complexes, **9** is thermally robust, resisting decomposition upon heating to 115 °C for several days. Notably, further heating to 160 °C liberates alkane and forms unidentified zirconium(IV) products, which yield ammonium chloride upon treatment with excess HCl.

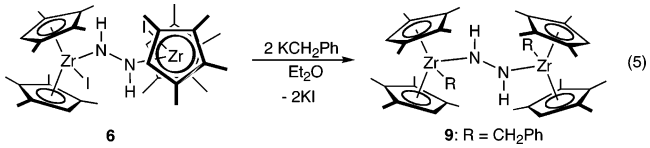

(5)

Confirmation of the diazenido ligand hapticity was provided by X-ray diffraction. The molecular structure of **9** is presented in Figure 6 with selected metrical parameters reported in Table 6. In the solid state, the molecule contains a center of inversion, relating the cyclopentadienyl ligands on the two ends of the dimer as well as the transoid benzyl groups. In agreement with the solution ^{1}H NMR chemical shift, the diazenido ligand in **9** is end-on coordinated with a typical N−N bond length of 1.420(3) Å.

Attempts to prepare $[(\eta^5\text{-}C_5Me_4H)_2Zr(CH_2SiMe_3)]_2(\mu_2,\eta^1,\eta^1\text{-}N_2H_2)$ by alkylation of **6** with 2 equiv of $LiCH_2SiMe_3$ afforded $[(\eta^5\text{-}C_5Me_4H)_2ZrI][(\eta^5\text{-}C_5Me_4H)_2Zr(CH_2SiMe_3)](\mu_2,\eta^1,\eta^1\text{-}N_2H_2)$ (**10**), the product of a single salt metathesis (eq 6). Stirring either **6** or **10** with excess $LiCH_2SiMe_3$ did not result in substitution of the remaining iodide ligand. Characterization of **10** was accomplished by routine spectroscopic and analytic methods. One notable feature of the ^{1}H NMR spectrum of **10** is the observation of two downfield doublets ($^3J_{N-H}$ = 12 Hz) centered at 8.46 and 9.10 ppm for the hydrogens of the end-on bound diazenido ligand. Synthesis of the desired dialkylated product, $[(\eta^5\text{-}C_5Me_4H)_2Zr(CH_2SiMe_3)]_2(\mu_2,\eta^1,\eta^1\text{-}N_2H_2)$ (**11**), was accomplished by addition of 2 equiv of $LiCH_2SiMe_3$ to **8**

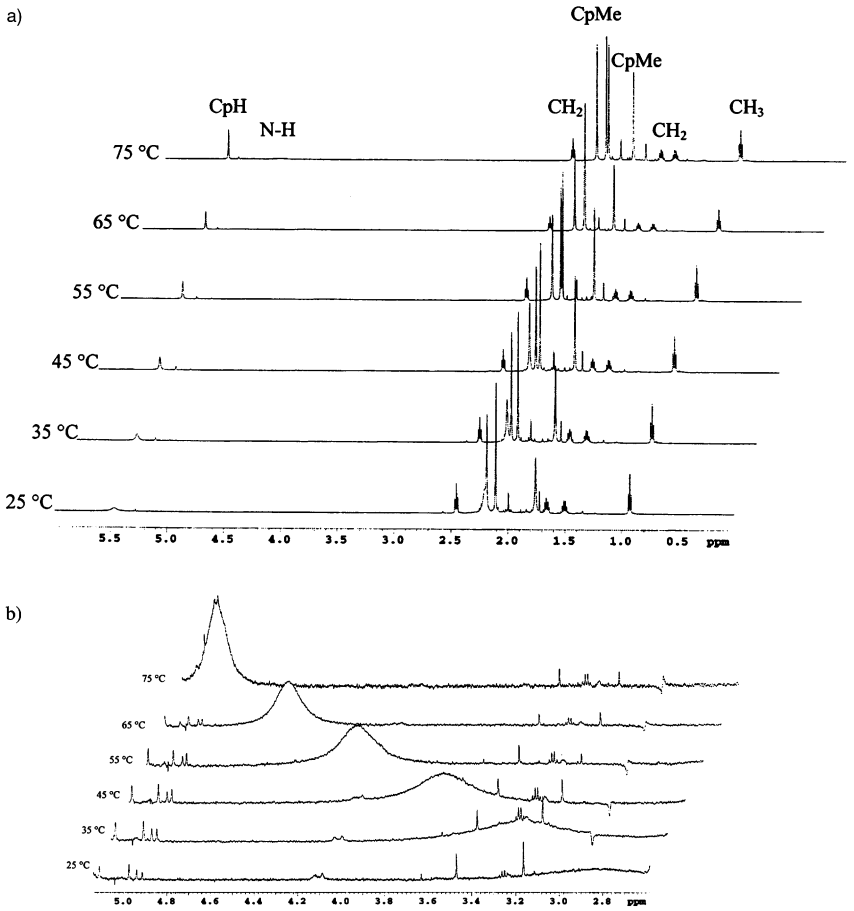

Figure 7. (a) Variable-temperature ^{1}H NMR spectra of **3** recorded in benzene-d_6. (b) The N−H region of the spectra.

(eq 6). A downfield N−H resonance is observed at 7.93 ppm, consistent with η^1,η^1 coordination of the $[N_2H_2]^{2-}$ ligand.

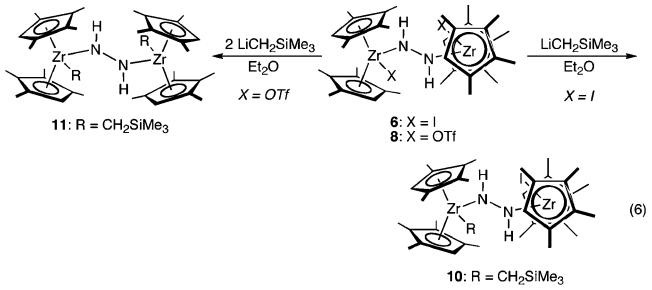

Attempts to introduce a smaller alkyl ligand such as methyl have not been successful. The hapticity of the diazenido and the migratory aptitude of the smaller alkyl upon thermolysis of $[(\eta^5\text{-}C_5Me_4H)_2Zr(CH_3)]_2(N_2H_2)$ were of interest. Unfortunately, treatment of **6** or **7** with 2 equiv of MeLi or MeMgBr furnished the zirconocene dimethyl complex, $(\eta^5\text{-}C_5Me_4H)_2Zr(CH_3)_2$,[31] while the same reaction with **8** produced no reaction. The fate of the diazenido ligand in the reactions with **6** and **7** is unknown.

Preparation of static zirconocene diazenido complexes such as **6**−**11** with end-on $[N_2H_2]^{2-}$ ligands provided insight into the solution dynamics of the acetylide zirconocene diazenido complexes, **3**−**5**. Each of the compounds was examined by variable-temperature NMR spectroscopy and exhibited similar ^{1}H NMR behavior as a function of temperature. As a result, only the variable-temperature profile (Figure 7) of **3** will be presented in detail. From 25 to 75 °C, the hexyl chain on the acetylide ligand and three cyclopentadienyl methyl groups appear sharp and are essentially invariant with temperature. The other methyl group is broad at 25 °C and steadily sharpens upon warming. Similar behavior is observed with the cyclopentadienyl hydrogen, where it appears as a very broad resonance at 25 °C and steadily narrows until a sharp peak is observed at 75 °C. The most significant feature of the variable-temperature spectra of **3** is the temperature dependence of the N−H chemical shift. At 25 °C, this peak appears as a very broad singlet centered at 2.85 ppm, consistent with η^2,η^2 hapticity of the $[N_2H_2]^{2-}$ ligand. This resonance steadily shifts downfield with increased temperature, finally appearing at 4.62 ppm at 75 °C, the highest temperature examined. The dynamic behavior of **3**−**5** can therefore be rationalized by a process whereby the $[N_2H_2]^{2-}$ ligand is interconverting between side-on and end-on hapticity. While the diazenido ligand is dynamic, the progressive downfield migration of the N−H resonance with increased temperature demonstrates an increased population of the end-on isomer upon warming (eq 7).

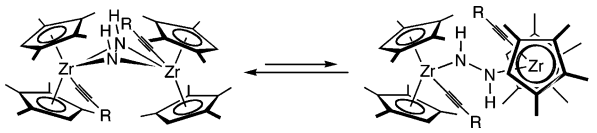

Solution ^{15}N NMR data also support the interconversion of the diazenido ligand as the origin of the dynamic behavior. At

(31) Chirik, P. J.; Day, M. W.; Bercaw, J. E. *Organometallics* **1999**, *18*, 1873.

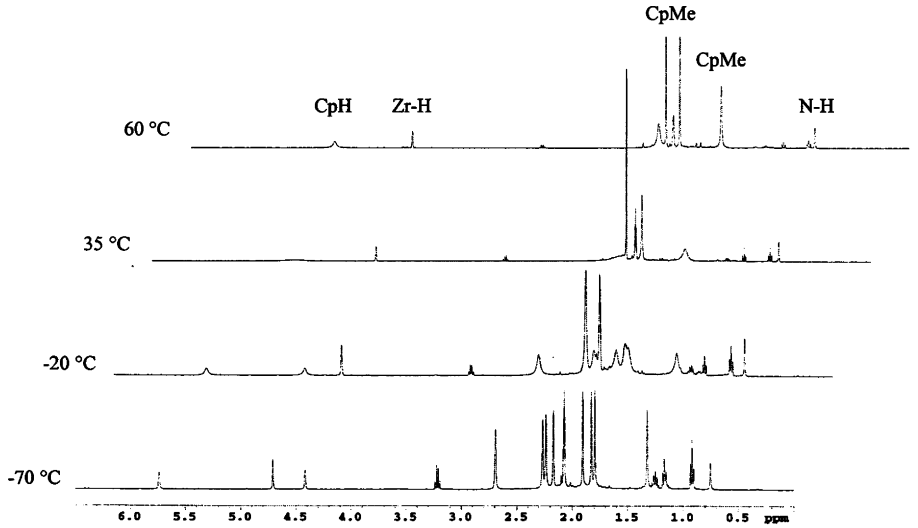

Figure 8. Variable-temperature ^{1}H NMR spectra of **2** recorded in toluene-d_8.

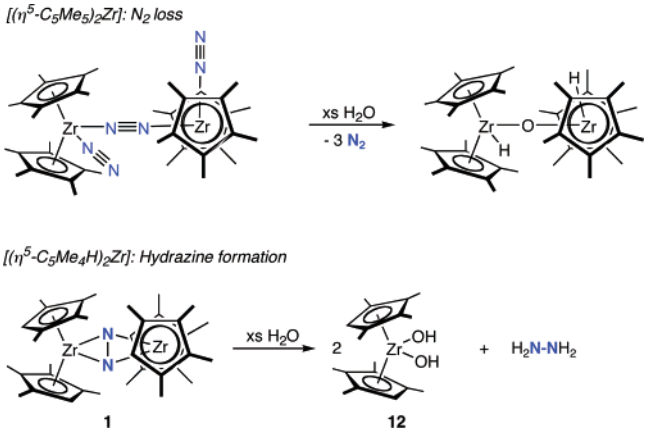

Figure 9. Hydrolysis of zirconocene dinitrogen complexes as a function of cyclopentadienyl ligand.

−78 °C, **4-^{15}N** exhibits a single ^{15}N resonance centered at 86.0 ppm, similar to the value of 74.6 ppm observed for **2-^{15}N** (Table 3), consistent with an η^2,η^2-$[N_2H_2]^{2-}$ ligand at this temperature. Warming the benzene-d_6 solution of **4-^{15}N** resulted in a gradual downfield shifting of the ^{15}N resonance, ultimately appearing at 224.4 ppm at 115 °C. This value is in excellent agreement with the chemical shift of 285.9 ppm observed for **6-^{15}N**, a complex that contains a static η^1,η^1 $[N_2H_2]^{2-}$ core.

Observation of the interconversion of the hapticity of the diazenido ligands in **3**−**5** prompted a similar variable-temperature NMR study with **2**. We previously reported[20] that the ^{1}H NMR spectrum of **2** recorded at 22 °C was suggestive of dynamic behavior, exhibiting broadened resonances for the cyclopentadienyl hydrogen and two of the cyclopentadienyl methyl groups. At this temperature, only one set of ligand resonances is observed with the two portions of the dimer being equivalent. Cooling a toluene-d_8 solution of **2** to −70 °C lowers the symmetry of the complex, producing a spectrum with eight cyclopentadienyl methyl peaks, two cyclopentadienyl hydrogens, and singlets for the N−H and Zr−H (Figure 8). Warming the solution to 60 °C produced a single, slightly broadened cyclopentadienyl resonance and four cyclopentadienyl methyl peaks, although two are significantly broadened. Importantly, both the N−H and the Zr−H resonances are essentially unchanged, both in peak shape and in chemical shift, over the range of temperatures studied. Furthermore, the ^{15}N NMR spectra are essentially invariant; a singlet is observed at 74.6 ppm at −78 °C that shifts only slightly to 78.7 ppm upon warming to 75 °C. These data demonstrate that a change in hapticity of the $[N_2H_2]^{2-}$ on the NMR time scale is unlikely and that the dynamic process probably arises from nitrogen inversion in the diazenido core (eq 8). The presence of small, σ-only ligands such as hydride shift the equilibrium to favor the formally 18 electron, side-on isomer. Although the end-on isomer is not sufficiently populated to be observed by NMR spectroscopy, it has been implicated in isotopic exchange reactions involving isotopologues of **2**,[19,20] suggesting that it is kinetically accessible.

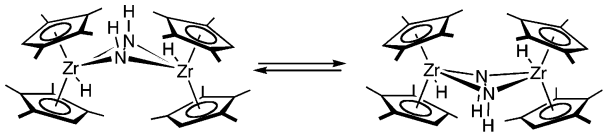

Dinitrogen Functionalization by Treatment with Electrophiles. The reactivity of the dinitrogen ligand in **1** was also explored with electrophilic reagents with the goal of functionalizing N_2 by proton transfer. Transformations of this type would complement the cycloaddition pathway observed with H_2 and terminal alkynes. We have previously reported that addition of HCl to **1** yields hydrazine,[20] in analogy to Bercaw's seminal N_2H_4 synthesis from $[(\eta^5\text{-}C_5Me_5)_2Zr(\eta^1\text{-}N_2)]_2(\mu_2,\eta^1,\eta^1\text{-}N_2)$.[10] Significantly, addition of a weaker Brønsted acid such as water to **1** also produced N_2H_4 along with $(\eta^5\text{-}C_5Me_4H)_2Zr(OH)_2$ (**12**, Figure 9). This result contrasts the chemistry observed with $[(\eta^5\text{-}C_5Me_5)_2Zr(\eta^1\text{-}N_2)]_2(\mu_2,\eta^1,\eta^1\text{-}N_2)$, where treatment with H_2O furnished $[(\eta^5\text{-}C_5Me_5)_2ZrH]_2(\mu_2\text{-}O)$ with loss of free N_2.[32]

Attempts to observe a hydroxy zirconocene diazenido intermediate during the aqueous protonation of **1** have been unsuccessful, as addition of substoichiometric amounts of H_2O resulted in only partial conversion to **12** and N_2H_4. Formation of hydrazine from coordinated dinitrogen by addition of H_2O prompted investigation of other proton sources for N−H bond assembly. It was hypothesized that similar reagents would also allow observation of diazenido intermediates along the N_2

(32) Hillhouse, G. L.; Bercaw, J. E. *J. Am. Chem. Soc.* **1984**, *106*, 5472.

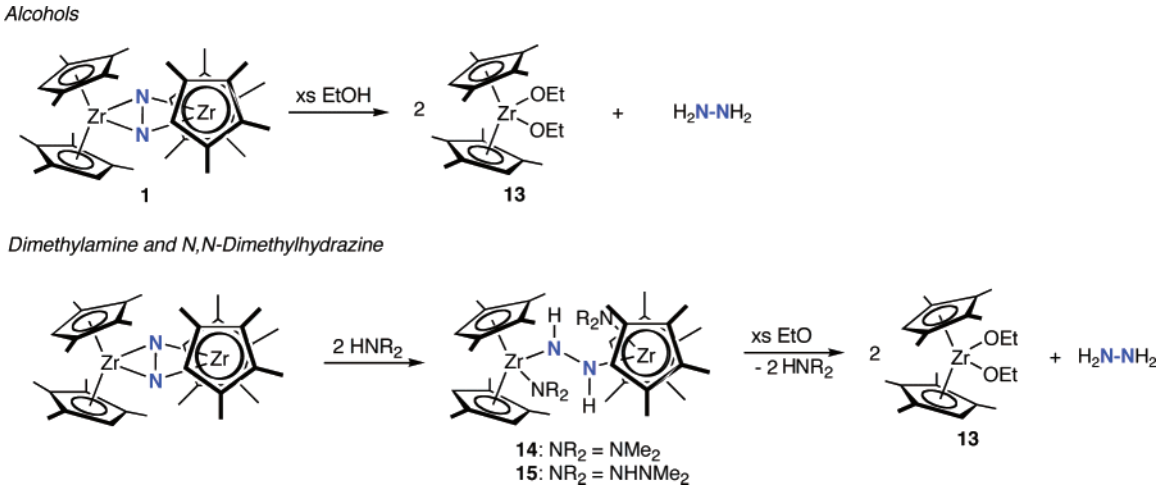

Figure 10. Dinitrogen functionalization by proton transfer.

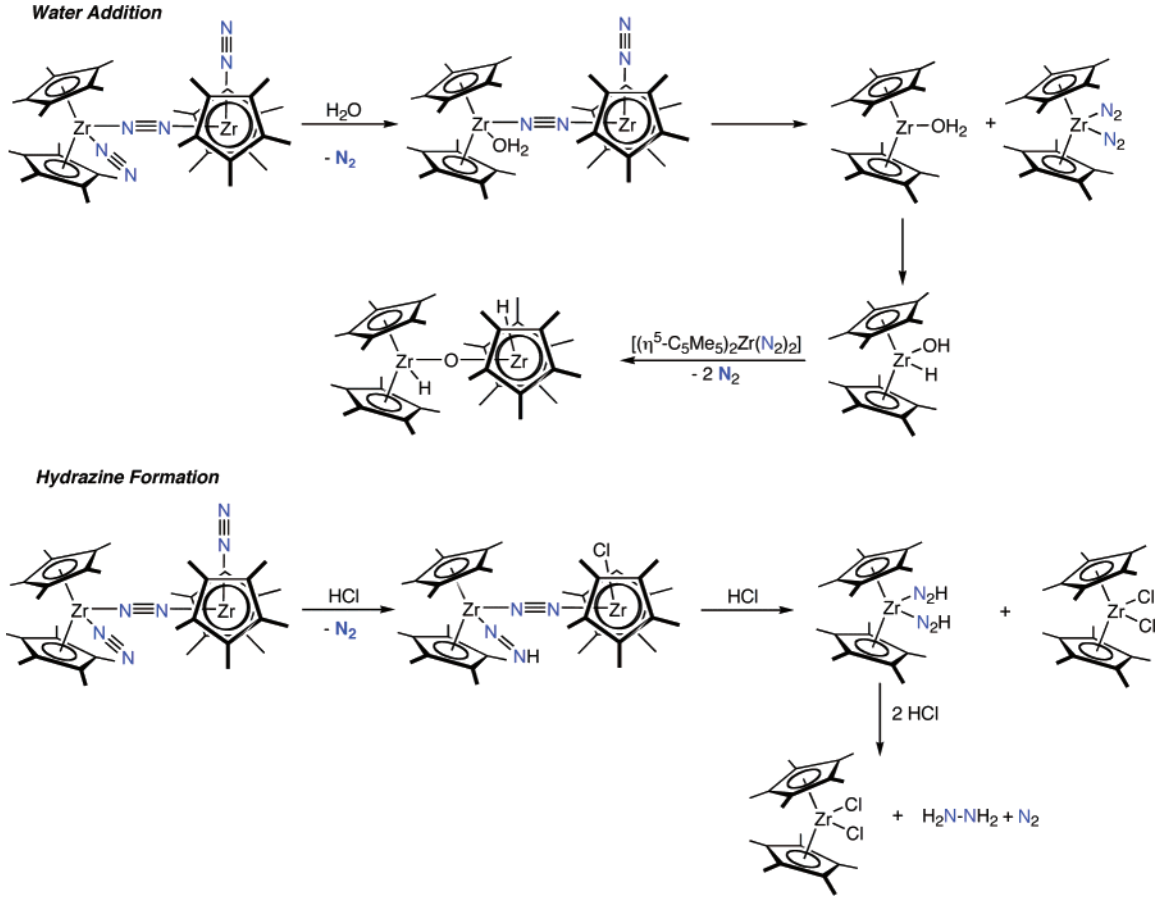

Figure 11. Mechanistic comparison for protonation reactions in zirconocene dinitrogen complexes.

functionalization pathway. Careful addition of 2 equiv of anhydrous ethanol to **1** induced partial conversion to (η^5-$C_5Me_4H)_2Zr(OEt)_2$ (**13**) along with free hydrazine. Other unidentified zirconium compounds are also observed using this procedure. However, clean conversion of **1** to **13** and N_2H_4 was accomplished by addition of a slight excess (~5 equiv) of ethanol (Figure 10).

Coordination of a primary or secondary amine to an electrophilic early transition metal center is known to increase the acidity of the N−H bond and facilitate proton transfer,[31] suggesting that amines and hydrazines could protonate coordinated dinitrogen and allow observation of an amido or hydrazido zirconocene diazenido complex. Given the similar pK_a values of the conjugate acids of the free amines or hydrazines and the zirconium diazenido ligand, it was anticipated that the reaction would afford the $[N_2H_2]^{2-}$ complex and not liberate free hydrazine. As expected, addition of excess $HNMe_2$ or H_2NNMe_2 to **1** furnished $[(\eta^5\text{-}C_5Me_4H)_2Zr(NMe_2)]_2(\mu_2,\eta^1,\eta^1\text{-}N_2H_2)$ (**14**) and $[(\eta^5\text{-}C_5Me_4H)_2Zr(NHNMe_2)]_2(\mu_2,\eta^1,\eta^1\text{-}N_2H_2)$ (**15**), respectively (Figure 10). In benzene-d_6, sharp N−H resonances are observed at 8.21 (**14**) and 7.03 ppm (**15**), respectively, diagnostic of static, η^1,η^1-$[N_2H_2]^{2-}$ ligands. Liberation of hydrazine was

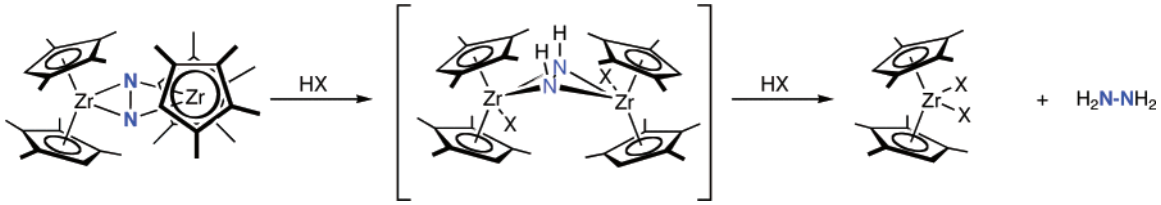

Figure 12. Proposed mechanism for hydrazine formation from **1** by treatment with proton donors.

accomplished by treatment of **14** or **15** with excess ethanol, thus demonstrating the competency of diazenido intermediates in the formal reduction of N_2 to hydrazine (Figure 10).

The ability of **1** to undergo protonation to yield N_2H_4 with weak acids underscores the influence of cyclopentadienyl substituents on transformations involving coordinated dinitrogen. The difference in reactivity between **1** and $[(\eta^5\text{-}C_5Me_5)_2Zr(\eta^1\text{-}N_2)]_2(\mu_2,\eta^1,\eta^1\text{-}N_2)$ can be traced to the steric environments about the two zirconium centers. For the more sterically hindered permethylated zirconocene, Bercaw[32] proposed the mechanism shown in Figure 11 to account for the observed loss of dinitrogen upon addition of water. Initial substitution of a terminal N_2 ligand by H_2O induces scission of the dimer to yield a transient, monomeric bis(dinitrogen) complex, $(\eta^5\text{-}C_5Me_5)_2Zr(\eta^1\text{-}N_2)_2$, and the zirconium(II) water adduct, $(\eta^5\text{-}C_5Me_5)_2Zr(OH_2)$. Experimental support for an 18-electron bis(dinitrogen) complex has recently been provided by our laboratory with the isolation and crystallographic characterization of the titanium congeners, $(\eta^5\text{-}C_5Me_4R)_2Ti(\eta^1\text{-}N_2)_2$ ($R = CHMe_2$, CMe_3, $SiMe_3$).[33] Formation of $[(\eta^5\text{-}C_5Me_5)_2ZrH]_2(\mu_2\text{-}O)$ is then accomplished by α-elimination in the water adduct followed by trapping by the bis(dinitrogen) complex.

Treatment of $[(\eta^5\text{-}C_5Me_5)_2Zr(\eta^1\text{-}N_2)]_2(\mu_2,\eta^1,\eta^1\text{-}N_2)$ with stronger acids such as HCl does indeed yield hydrazine. Based on the stoichiometry of the reaction and isotopic labeling studies, Bercaw[34] proposed the pathway shown in Figure 11 involving protonation of both the terminal and the bridging dinitrogen ligands. Importantly, both pathways involve the formation of monomeric intermediates, a consequence of the steric environment imparted by the bulky pentamethylcyclopentadienyl ligand.

The η^2,η^2 hapticity of the N_2 ligand in **1** coupled with twisting of the dimer results in increased back-bonding and as a consequence yields a formal $[N_2]^{4-}$ ligand.[19] In $[(\eta^5\text{-}C_5Me_5)_2Zr(\eta^1\text{-}N_2)]_2(\mu_2,\eta^1,\eta^1\text{-}N_2)$, the dinitrogen ligands are not significantly elongated from free N_2, behaving more like neutral donors than hydrazido fragments. The increased electron density of the formal $[N_2]^{4-}$ core in **1** renders the dinitrogen ligand sufficiently basic to undergo protonation by weak Brønsted acids. In other words, the formal four-electron reduction of N_2 by the two zirconocenes, made possible by side-on coordination, allows metathetical synthesis of N_2H_4 in contrast to the permethylzirconocene system, where hydrazine formation can be viewed in analogy to Chatt-type N_2 reduction schemes. Furthermore, the reduced steric bulk imparted by the $[C_5Me_4H]$ ligand also allows formation of dimeric zirconocene diazenido compounds, which are key intermediates on the protonolysis pathway (Figure 12).

Concluding Remarks

Functionalization of the side-on bound, activated dinitrogen ligand in $[(\eta^5\text{-}C_5Me_4H)_2Zr]_2(\mu_2,\eta^2,\eta^2\text{-}N_2)$ to afford zirconocene diazenido complexes, $[(\eta^5\text{-}C_5Me_4H)_2ZrX]_2(\mu_2\text{-}N_2H_2)$, has been accomplished by addition of terminal alkynes, dimethylamine and *N*,*N*-dimethylhydrazine. The hapticity of the $[N_2H_2]^{2-}$ core depends on the size of the anionic ligand in the zirconocene wedge − smaller donors such as hydride yield diazenido complexes that are predominantly side-on bound, whereas intermediate size acetylide ligands afford compounds where the interconversion between the two hapticities is facile in solution and population of the end-on isomer becomes more significant at higher temperatures. Larger donors such as chloride, iodide, triflate, or alkyl produce diazenido complexes that are exclusively η^1,η^1 coordinated in both the solid state and in solution. It should be noted that in the case of the halides and the triflato compounds, the influence of π-donation on the preferred hapticity cannot be discounted. Regardless of coordination mode, the diazenido compounds are intermediates in the reduction of dinitrogen to hydrazine, as treatment with ethanol yields N_2H_4. The protonation results observed with $[(\eta^5\text{-}C_5Me_4H)_2Zr]_2(\mu_2,\eta^2,\eta^2\text{-}N_2)$ contrasts related chemistry with $[(\eta^5\text{-}C_5Me_5)_2Zr(\eta^1\text{-}N_2)]_2(\mu_2,\eta^1,\eta^1\text{-}N_2)$, where the weakly activated, end-on bound dinitrogen ligands are readily displaced as free N_2 upon treatment with water. These results establish the importance of side-on coordination of the N_2 ligand for the construction of N−H bonds either by cycloaddition or protonolysis pathways and further highlight the critical role cyclopentadienyl substituents play in zirconocene dinitrogen chemistry.

Experimental Section[35]

Preparation of $[(\eta^5\text{-}C_5Me_4H)_2Zr(C{\equiv}C^tBu)]_2(\mu_2,\eta^2,\eta^2\text{-}N_2H_2)$ (4). A 25 mL round-bottomed flask was charged with 0.080 g (0.115 mmol) of $[(\eta^5\text{-}C_5Me_4H)_2Zr]_2(\mu_2,\eta^2,\eta^2\text{-}N_2)$ (**1**) and approximately 10 mL of pentane. The dark green solution was frozen at −196 °C, and 21 Torr (0.23 mmol) of *tert*-butyl acetylene was admitted via a 100.1 mL calibrated gas bulb on a high vacuum line. The resulting dark red solution was stirred at ambient temperature for 2 h. After this time, the solvent was removed in vacuo leaving a white powder. Recrystallization from diethyl ether layered with pentane at −35 °C afforded 0.085 g (86%) of **4** as colorless crystals. Anal. Calcd for $C_{48}H_{72}Zr_2N_2$: C, 67.07; H, 8.44; N, 3.26. Found: C, 66.93; H, 8.72; N, 2.94. ^{1}H NMR (benzene-d_6, 20 °C): $\delta = 1.41$ (s, 18H, C*Me*$_3$), 1.69 (br s, 16H, C$_5$*Me*$_4$H), 2.09 (br s, 16H, C$_5$*Me*$_4$H), 2.18 (br s, 16H, C$_5$*Me*$_4$H), 5.42 (br s, 4H, C$_5$Me$_4$*H*). ^{1}H NMR (benzene-d_6, 80 °C): $\delta = 1.37$ (s, 18H, C*Me*$_3$), 1.85 (s, 12H, C$_5$*Me*$_4$H), 2.08 (s, 12H, C$_5$*Me*$_4$H), 2.10 (s, 12H, C$_5$*Me*$_4$H), 2.18 (s, 12H, C$_5$*Me*$_4$H), 4.80 (br s, 2H, N-*H*), 5.42 (br s, 4H, C$_5$Me$_4$*H*). ^{13}C{^{1}H} NMR (benzene-d_6, 23 °C): $\delta = 12.65$, 13.90, 29.26 (C$_5$*Me*$_4$H), 32.93 (C*Me*$_3$), 123.16, 124.08 (Cp). ^{15}N NMR (toluene-d_8, −78 °C): $\delta = 86.0$. ^{15}N NMR (toluene-d_8, 115 °C): $\delta = 224.4$. IR (KBr): $\nu_{N-H} = 3297$ cm^{-1}, $\nu_{C\equiv C} = 2079$ cm^{-1}.

(33) Hanna, T. E.; Lobkovsky, E.; Chirik, P. J. *J. Am. Chem. Soc.* **2004**, *126*, 14688.
(34) Manriquez, J. M.; Sanner, R. D.; Marsh, R. E.; Bercaw, J. E. *J. Am. Chem. Soc.* **1976**, *98*, 3042.

(35) General considerations and additional experimental procedures are contained in the Supporting Information.

Preparation of $[(\eta^5\text{-}C_5Me_4H)_2ZrI]_2(\mu_2,\eta^1,\eta^1\text{-}N_2H_2)$ (6). A thick walled reaction vessel was charged with 0.050 g (0.072 mmol) of $[(\eta^5\text{-}C_5Me_4H)_2ZrH]_2(\mu_2,\eta^2,\eta^2\text{-}N_2H_2)$ (**2**) and approximately 10 mL of toluene. On the vacuum line, the vessel was chilled to −196 °C and evacuated. At this temperature, 70 Torr (0.36 mmol) of CH_3I was admitted to the vessel via a 100.1 mL calibrated gas bulb. The resulting reaction mixture was warmed to ambient temperature and stirred for 2 h forming a deep purple solution. The solvent was removed in vacuo, yielding a dark purple oil which was washed several times with pentane to afford 0.068 g (95%) of a dark purple solid identified as **6**. Single crystals suitable for X-ray diffraction were obtained from a concentrated benzene solution. Anal. Calcd for $C_{36}H_{54}I_2N_2Zr_2$: C, 45.46; H, 5.72; N, 2.95. Found: C, 44.97; H, 5.88; N, 2.65. ^{1}H NMR (benzene-d_6): δ = 1.81 (s, 12H, C_5Me_4H), 1.99 (s, 12H, C_5Me_4H), 2.13 (s, 12H, C_5Me_4H), 2.21 (s, 12H, C_5Me_4H), 5.51 (s, 4H, C_5Me_4H), 8.90 (s, 2H, N-*H*). ^{13}C{^{1}H} NMR (benzene-d_6): δ = 12.87, 13.66, 14.78, 15.65 (C_5Me_4H), 109.92, 116.45, 118.94, 122.67, 124.19 (Cp). ^{15}N NMR (benzene-d_6): δ = 285.9. IR (KBr): ν_{N-H} = 3327 cm^{-1}. IR (benzene-d_6): ν_{N-H} = 3237 cm^{-1}. IR (benzene-d_6): ν_{N-D} = 2312 cm^{-1}.

Preparation of $[(\eta^5\text{-}C_5Me_4H)_2Zr(CH_2Ph)]_2(\mu_2,\eta^1,\eta^1\text{-}N_2H_2)$ (9). A 20 mL scintillation vial was charged with 0.175 g (0.184 mmol) of $[(\eta^5\text{-}C_5Me_4H)_2ZrI]_2(\mu_2,\eta^1,\eta^1\text{-}N_2H_2)$ (**6**) and approximately 15 mL of diethyl ether. The resulting dark purple solution was chilled to −32 °C and treated with 0.052 g (0.405 mmol) of KCH_2Ph. The reaction mixture was stirred at ambient temperature for 36 h, slowing turning dark red. After this time, the reaction mixture was filtered through Celite and the solvent removed in vacuo and washed with pentane and cold diethyl ether to afford 0.107 g (66%) of a red powder identified as **9**. Crystals suitable for X-ray diffraction were obtained from a concentrated benzene solution. Anal. Calcd for $C_{50}H_{68}N_2Zr_2$: C, 68.28; H, 7.79; N, 3.18. Found: C, 68.16; H, 7.64; N, 2.78. ^{1}H NMR (benzene-d_6, 20 °C): δ = 1.83 (s, 12H, C_5Me_4H), 1.84 (s, 12H, C_5Me_4H), 1.88 (s, 12H, C_5Me_4H), 1.90 (s, 12H, C_5Me_4H), 5.31 (s, 4H, C_5Me_4H), 6.94 (t, 4H, 8 Hz, *m*-Ar), 7.21 (d, 4H, 5 Hz, *o*-Ar), 7.30 (t, 4H, 2 Hz, *p*-Ar), 8.14 (s, 2H, N-*H*). ^{13}C{^{1}H} NMR (benzene-d_6, 20 °C): δ = 12.21, 12.44, 13.30, 13.72 (C_5Me_4H), 51.75 (CH_2Ar), 109.68, 116.85, 120.11, 121.46 (Cp), 116.06, 121.23, 155.11 (Ar). IR (KBr): ν_{N-H} = 3344 cm^{-1}.

Acknowledgment. We thank the National Science Foundation (CAREER Award to P.J.C.), Research Corporation (Cottrell Scholarship), and the Packard Foundation for financial support. Cambridge Isotope Laboratories is also acknowledged for a generous gift of $^{15}N_2$.

Supporting Information Available: Additional experimental procedures, the spectral simulation of **6-^{15}N**, and crystallographic data for **4**, **6**, **7**, **8**, and **9**. This material is available free of charge via the Internet at http://pubs.acs.org.

JA050387B